THE JOURNAL OF PHYSICAL CHEMISTRY A

ARTICLE

pubs.acs.org/JPCA

Kinetics of the Self Reaction of Cyclohexyl Radicals

Ksenia A. Loginova and Vadim D. Knyazev*

Research Center for Chemical Kinetics, Department of Chemistry, The Catholic University of America, Washington, DC 20064, United States

Supporting Information

ABSTRACT: The kinetics of the self-reaction of cyclohexyl radicals was studied by laser photolysis/photoionization mass spectroscopy. Overall rate constants were obtained in direct real-time experiments in the temperature region 303 − 520 K and at bath gas (helium with up to 5% of radical precursors) densities (3.00−12.0) × 10^{16} molecules cm^{-3}. Cyclohexyl radicals were produced by a combination of the 193 nm photolysis of oxalyl chloride ($(CClO)_2$) with the subsequent fast reaction of Cl atoms with cyclohexane, and their initial concentrations were determined from real-time profiles of HCl. The observed overall c-C_6H_{11} + c-C_6H_{11} rate constants demonstrate negative temperature dependence, which can be described by the following expressions: k_1 = 4.8 × 10^{-12} exp(+542 K/T) cm^3 $molecule^{-1}$ s^{-1}, with estimated uncertainty of 16% over the 303−520 K temperature range. The fraction of disproportionation equal to 41 ± 7% was determined at 305 K; analysis of earlier experimental determinations of the disproportionation-to-recombination branching ratio leads to recommending this room-temperature value for other temperatures. The corresponding temperature dependences of the recombination (1a, bicyclohexyl product) and the disproportionation (1b, cyclohexene and cyclohexane products) channels are k(1a) = 2.8 × 10^{-12} exp(+542 K/T) and k(1b) = 2.0 × 10^{-12} exp(+542 K/T) cm^3 $molecule^{-1}$ s^{-1}, with estimated uncertainties of 20% and 29%, respectively.

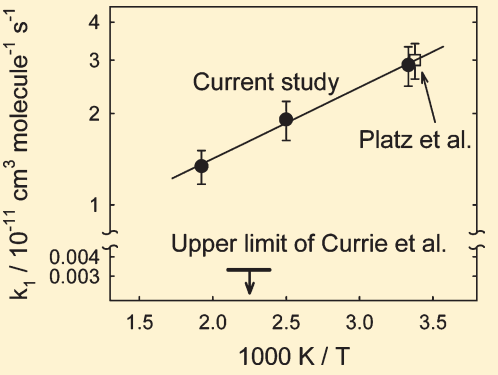

I. INTRODUCTION

Radical−radical reactions are important elementary steps in the combustion and pyrolysis of hydrocarbons.[1,2] These reactions generally, although not without exceptions, serve as chain termination pathways. Knowledge of the rate constant and the channel branching ratio of such reactions is necessary for accurate modeling of the combustion of organic fuels. Despite their importance, information available on the rates of these reactions is sparse and often controversial as radical−radical reactions are difficult to study experimentally due to the high reactivity of the species involved. Because of the difficulties encountered in experimental studies, theoretical methods of evaluating and predicting rates of radical−radical reactions become ever more important, and recent advancement of theoretical methods holds great promise (e.g., refs 3 and 4 and references cited therein). Further development and validation of theoretical methods requires a set of accurately measured experimental data on a variety of benchmark reactions, preferably obtained in direct experiments. Such a database is generally lacking, and in particular there is a scarcity of rate data for the reactions between relatively large radicals.

Experimental difficulties in direct experimental studies of radical−radical kinetics are generally caused by two factors. One is the difficulty in creating requisite radicals in the gas phase without at the same time creating some other undesired reactive species, the reactions of which may interfere with the subsequent kinetics of the radicals under study. The second factor is the difficulty in determining the initial concentrations of the radicals formed, as any potential error in signal calibration is directly translated into an error in the determined rate constant. In that respect, photolytic decomposition of various precursors frequently fails as a "clean" source of radicals, especially when radicals in question contain more than one or two carbon atoms and at elevated temperatures (e.g., ref 5). A successfully used alternative is pulsed production of chlorine or fluorine atoms that are made to quickly react with a corresponding hydrocarbon to produce the desired radicals (e.g., refs 5−8). In the current study, the reaction between Cl atoms and cyclohexane is used as a "clean" source of cyclohexyl radicals, and the second product of this reaction, HCl, serves as a nonreactive (under the conditions of experiments performed in this work) measure of the amount of radicals produced.

The self-reaction of cyclohexyl radicals

$$c\text{-}C_6H_{11} + c\text{-}C_6H_{11} \rightarrow C_{12}H_{22}\ (\text{bicyclohexyl}) \quad (1a)$$

$$\rightarrow c\text{-}C_6H_{10} + c\text{-}C_6H_{12} \quad (1b)$$

can proceed via recombination (channel 1a) or disproportionation (channel 1b). The recombination-to-disproportionation branching has been studied before by several groups.[9−12] All studies used gas chromatography or gas chromatography−mass spectrometry to analyze final products. The range of reported values of branching fractions of the disproportionation channel

Received: April 29, 2011
Revised: June 17, 2011
Published: June 26, 2011

1b is 31−54% and the experimental temperatures are from 302 to 475 K.

Two experimental determinations of the rate constant of reaction 1 are available in the literature. Currie et al.[10] in 1974 obtained an upper limit of 1.7×10^{-14} cm^3 molecule^{-1} s^{-1} for the rate constant of the recombination channel (1a) using 360 nm photolysis and final product analysis. Combined with the branching ratio of $k_{1b}/k_{1a} = 0.99$ reported in the same paper, this results in the upper limit of $\sim 3 \times 10^{-14}$ cm^3 molecule^{-1} s^{-1} for the rate constant of the overall reaction. In 1999, Platz et al.[6] used pulsed radiolysis of SF_6/cyclohexane mixtures to create c-C_6H_{11} and UV absorption to monitor their kinetics in real-time experiments. These authors obtained the value of $k_1 = (3.0 \pm 0.4) \times 10^{-11}$ cm^3 molecule^{-1} s^{-1} at 296 K and the pressure of 700 Torr of nitrogen.

In this work, we present the results of the first direct real-time experimental investigation of the temperature dependence of the kinetics of the self-reaction of cyclohexyl radicals. Reaction 1 was studied by Laser Photolysis/Photoionization Mass Spectrometry. Overall rate constants of reaction 1 were obtained in the temperature interval 303−520 K and bath gas (helium with up to 5% of radical precursors) densities in the range $(3.00-12.0) \times 10^{16}$ molecules cm^{-3}. The branching fraction of channel 1b was obtained at room temperature and a bath gas density of 12.0×10^{16} molecules cm^{-3}. The article is organized as follows: section II presents the experimental methods and the results of the determinations of the rate constants and the branching fraction of disproportionation, and a discussion is presented in section III.

II. EXPERIMENTAL SECTION

Apparatus. Details of the experimental apparatus have been described previously;[13] only a brief description is given here. Pulsed 193 nm unfocused light from a Lambda Physik 201 MSC excimer laser was directed along the axis of a heated 50-cm-long tubular reactor (i.d. 1.05 cm). The reactor surface was coated with boron oxide to reduce radical wall losses.[14] The laser was operated at 4 Hz and a fluence of 10−80 mJ pulse^{-1}. In order to replace the photolyzed gas mixture with fresh reactants between laser pulses, the flow of the gas mixture containing the radical precursors and the bath gas (helium) was set at $\sim$4 m s^{-1}. The mixture was continuously sampled through a small tapered orifice in the wall of the reactor and formed into a beam by a conical skimmer before entering the vacuum chamber containing the photoionization mass spectrometer. As the gas beam traversed the ion source, a portion was photoionized by an atomic resonance lamp, mass selected by a quadrupole mass filter, and detected by a Daly detector. Temporal ion signal profiles were recorded from a short time before the laser pulse (10−30 ms) to 15−30 ms following the pulse by a multichannel scaler interfaced to a PC computer. Typically, data from 500 to 30 000 repetitions of the experiment were accumulated before the data were analyzed. The sources of the photoionization radiation were chlorine (8.9−9.1 eV, CaF_2 window, used to detect c-C_6H_{11}, c-C_6H_{10}, and benzene), hydrogen (10.2 eV, MgF_2 window, used to detect $C_{12}H_{22}$), and neon (16 eV, collimated hole structure, used to detect HCl, benzene, and $(CClO)_2$) resonance lamps.

Radical Generation. Real-time experimental studies of radical self-reactions, ideally, require a suitable pulsed source of radicals that should satisfy two requirements: (1) that the radicals of interest are the only reactive species present in the reactor during the kinetics of radical decay and (2) that the initial concentration of radicals can be determined with a high degree of accuracy. In the current study, the method of Baklanov and Krasnoperov[7] was used to generate cyclohexyl radicals. This method is based on using the 193 nm photolysis of oxalyl chloride ($(CClO)_2$) with consecutive conversion of Cl atoms to radicals of interest (R) and HCl by a fast reaction with a suitable substrate:

$$(CClO)_2 \xrightarrow{193\ nm} 2Cl + 2CO \quad (2a)$$

$$\rightarrow Cl + CO + CClO \rightarrow 2Cl + 2CO \quad (2b)$$

$$Cl + RH \rightarrow R + HCl \quad (3)$$

The 193 nm photolysis of oxalyl chloride serves as a "clean" photolytic source of chlorine atoms ("clean" in the sense that no other reactive species are produced by the photolysis). Since the yield of chlorine atoms in reaction 2 is exactly 200%, the initial concentration of Cl (and, consequently, that of R) can be determined either from the extent of the photolytic depletion of oxalyl chloride[8,15] or from the measured production of HCl.[8] The equivalence of the two methods of evaluating the initial concentration of Cl and R has been experimentally confirmed before.[8] In the experiments on the kinetics of reaction 1, the 193-nm photolysis of $(CClO)_2$ followed by the subsequent fast reaction of the Cl atoms with cyclohexane was used as a source of cyclohexyl radicals. Production of HCl was used to determine the initial concentrations of c-C_6H_{11}. Measured flows of (gaseous) HCl were used for calibration of the HCl ion signal. Concentrations of cyclohexane ($(2.0-11) \times 10^{14}$ molecules cm^{-3}) were selected to ensure a virtually instantaneous (on the time scale of the reactions studied) conversion of Cl into cyclohexyl radicals and HCl. The rate constant of reaction 3 is unknown but can be estimated at $(2-3) \times 10^{-10}$ cm^3 molecule^{-1} s^{-1} by analogy with the reactions of chlorine atoms with other alkanes (e.g., ref 16). The rate of the reverse reaction, that of c-C_6H_{11} with HCl, is negligibly small under the conditions of the current study, as can be expected on the basis of the known kinetics of the reaction of methyl radical with HCl (rate constants in the range $(0.5-1.2) \times 10^{-13}$ cm^3 molecule^{-1} s^{-1} between 300 and 495 K[17]). The observed temporal profiles of the HCl signal were flat during the 0−30 ms monitoring time, with temporal resolution determined by the per-channel dwell time of the multichannel scaler (0.1 − 0.3 ms). Separate experiments were performed to verify that no cyclohexyl radicals were produced by the photodissociation of cyclohexane in the absence of oxalyl chloride.

Radical precursors and other chemicals used (see below) were obtained from Aldrich (oxalyl chloride, ≥99%, cyclohexane, 99.9%), Alpha Aesar (cyclohexene, 99%), Matheson (HCl, 99.99%), Fisher Scientific (benzene, ≥99%), and Roberts Oxygen (helium, 99.999%, less than 0.0002% of oxygen). Oxalyl chloride, cyclohexane, cyclohexene, and benzene were purified by vacuum distillation prior to use. Helium and hydrogen chloride were used without further purification.

Determination of the Rate Constant. The kinetics of the cyclohexyl radical decay was monitored in real time. Rate constant measurements were performed using a technique applied by us earlier to the studies of the self-reactions of ethyl[5] and propargyl[8] radicals, which, in turn, is based on the method used by Slagle and co-workers[18] in their study of the $CH_3 + CH_3$ reaction. The experimental conditions were selected in such a way that the characteristic time of the reaction between Cl and cyclohexane was at least 300 times shorter (typically, 1000

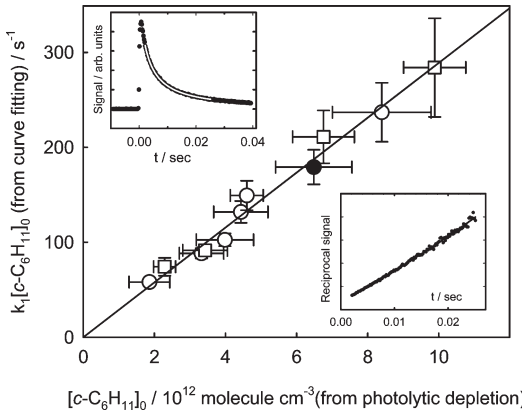

Figure 1. The $k_1[c\text{-}C_6H_{11}]_0$ versus $[c\text{-}C_6H_{11}]_0$ dependence obtained in the study of reaction 1 at room temperature. Circles: bath gas density of 12.0×10^{16} molecules cm^{-3}; squares: bath gas density of 3.0×10^{16} molecules cm^{-3}. Upper left inset shows a typical temporal $c\text{-}C_6H_{11}$ ion signal profile recorded in an experiment to determine the rate of the $c\text{-}C_6H_{11}$ + $c\text{-}C_6H_{11}$ reaction. The conditions are those of the filled circle on the main plot; the white solid line is the result of the fit with eq I. The lower right inset shows the reciprocal of the $c\text{-}C_6H_{11}$ ion signal as a function of time (also given in full size in the Supporting Information, Figure 1S). The observed slight deviation from linearity is due to the minor heterogeneous loss of radicals in reaction 4, as discussed in text.

times shorter) than that of the self-reaction of the cyclohexyl radicals. Under these experimental conditions, the self-reaction of $c\text{-}C_6H_{11}$ was unperturbed by any side processes and the only additional sink of the radicals was due to the heterogeneous wall loss, which was taken into account in the analysis. Thus, the experimental kinetic mechanism included reactions

$$c\text{-}C_6H_{11} + c\text{-}C_6H_{11} \rightarrow \text{products} \quad (1)$$

$$c\text{-}C_6H_{11} \rightarrow \text{wall loss} \quad (4)$$

For this kinetic mechanism and initial conditions described above, the corresponding first-order differential equations can be solved analytically:

$$S = \frac{S_0 \cdot k_4}{(2k' + k_4) \cdot e^{k_4 t} - 2k'} \quad (I)$$

Here, $k' = k[R]_0$, k_1 and k_4 are the rate constants of reactions 1 and 4, respectively, $[R]_0$ is the initial radical concentration, S is the radical ion signal, and S_0 is the signal amplitude. In each experiment, the values of the signal amplitude S_0, the wall loss rate k_4, and the $k_1[R]_0$ product were obtained from the fits of the real-time radical decay profile with eq I. A typical signal profile of the cyclohexyl radical decay is shown in Figure 1 (upper inset).

Different parts of the radical decay profiles exhibit different sensitivities to the fitting parameters. The initial part of the signal profile is most sensitive to the rate constant of the radical self-reaction, whereas the end part is most sensitive to the rate constant of the heterogeneous wall loss of the radicals. These sensitivities are illustrated in the lower inset in Figure 1, where the reciprocal of the radical signal (with the baseline determined before the photolyzing laser pulse subtracted) is plotted as a function of time. In the absence of any heterogeneous wall loss of radicals (pure second-order decay) the reciprocal signal is directly proportional to time and forms a straight line; the self-reaction rate constant can be obtained from the slope of the line. In the presence of heterogeneous loss, the line is curved, the initial slope is proportional to $(2k' + k_4)$, and the deviation from a straight line can serve as a measure of the contribution from the heterogeneous wall loss. As can be seen from the plot in Figure 1 (also, a full-sized plot of the same dependence is given in the Supporting Information), both the slope of the initial part of the reciprocal signal versus time dependence and the slight deviation from linearity are well characterized, which illustrates that both the $k_1[R]_0$ and the k_4 values can be obtained from the fit of the signal with a high degree of accuracy. Constraining the values of k_4 to the upper or lower limits of the resultant uncertainty ranges (1σ) generally resulted in fitted $k_1[R]_0$ values corresponding to the respective lower or upped error limits of the unconstrained fit.

The rate of the heterogeneous loss of radicals (reaction 4) did not display any dependence on the laser intensity or concentrations of the radical precursors, but was affected by the condition of the walls of the reactor, such as the history of exposure to different reacting mixtures. In principle, it was possible to obtain the rate constants of the heterogeneous loss of radicals, k_4, in separate experiments with low initial radical concentrations selected in such a way as to make the rates of radical self-reactions negligible. However, in the experiments performed to determine the rates of the $c\text{-}C_6H_{11}$ self-reaction (with high cyclohexyl concentrations), a small fraction of the Cl atoms produced in the photolysis of oxalyl chloride decayed on the reactor walls, which could possibly have affected the wall conditions. Thus, it was deemed more appropriate to determine the rates of wall losses of radicals in the same experiments where the rates of radical self-reactions were obtained. Separate experiments with low cyclohexyl concentrations (such that the $c\text{-}C_6H_{11}$ self-reaction was negligible) were performed to confirm that the values of k_4 obtained ($19-25\ s^{-1}$) are in general agreement with those derived from the three-parameter fits of radical decays obtained with high $c\text{-}C_6H_{11}$ concentrations ($5-24\ s^{-1}$). A reaction of the cyclohexyl radicals with oxygen impurity in the helium carrier gas may be a potential concern. However, under the experimental conditions used, the concentration of oxygen was less than 2.4×10^{11} molecules cm^{-3} (7−40 times lower than the initial concentrations of cyclohexyl), which makes any contribution of the $c\text{-}C_6H_{11} + O_2$ reaction to the overall kinetics of cyclohexyl decay negligible, especially considering the corresponding rate constant values of less than 1.7×10^{-11} cm^3 $molecule^{-1}$ s^{-1}.[20]

In each experiment, the initial concentration of the cyclohexyl radicals was determined by measuring the production of HCl relative to a calibration standard. This value was obtained directly from the HCl^+ ion profile. In each experiment to determine $k' = k_1[R]_0$, the production of HCl was measured two times (before and after the kinetics of the radical decay was recorded).

For each experimental temperature, the initial radical concentration $[R]_0$ ($R = c\text{-}C_6H_{11}$), was varied by changing the concentration of oxalyl chloride and/or the laser fluence. The values of the $k_1[R]_0$ product obtained from the data fits were plotted as a function of the initial concentration of radicals obtained from the measurements of the photolytic production of HCl ($[R]_0$). The values of the radical self-reaction rate constant were determined from the slopes of the linear $k_1[R]_0$ versus $[R]_0$ dependences. The regression fits were constrained to pass through the center of coordinates; however, unconstrained linear fits resulted in intercept values that were ~3 times smaller than the corresponding standard errors of the fit.

The values of the rate constant of reaction 1 were obtained at 303 (±4), 400, and 520 K. The upper experimental temperature

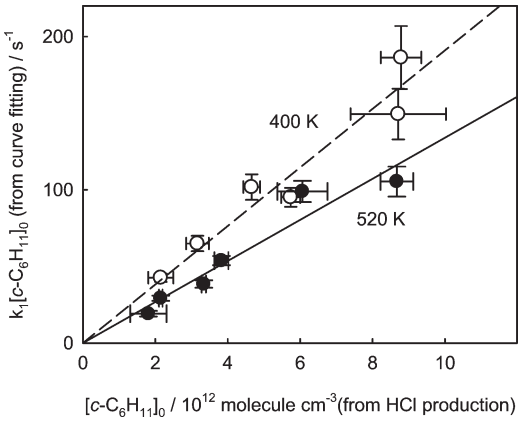

Figure 2. The $k_1[c\text{-}C_6H_{11}]_0$ versus $[c\text{-}C_6H_{11}]_0$ dependences obtained in the study of reaction 1 at 400 K (open circles and dashed line) and 520 K (filled circles and solid line).

was determined by the expected onset of the isomerization reaction proceeding via ring-opening and producing the methylcyclopentyl radical.[19,20] For this purpose, the value of 10 s^{-1} (similar to the typical rate of radical wall loss) was selected as the acceptable upper limit of the isomerization rate constant. RRKM/Master equation[21,22] calculations were performed to estimate isomerization rate constants using the G2(MP2)-level potential surface for cyclohexyl isomerization from the theoretical study of Knepp et al.[20] Calculations were performed using the ChemRate program.[23] The somewhat high value of the average energy transferred per deactivating collision, $\langle\Delta E\rangle_{down}$ = 500 cm^{-1}, was used, as it is safer to err on the higher side. The resultant isomerization rates were less than 1.4 s^{-1} at the experimental pressures and the highest temperature used in the current work, 520 K. A potential error in the energy barrier of 2 kcal mol^{-1} would result in a change of the isomerization rate constant at this temperature by a factor of 6.4. Thus, the upper limit of the isomerization rate at 520 K can be estimated at ~10 s^{-1}, which is significantly lower that the rates of cyclohexyl decay due to reaction 1. Hence, 520 K was selected as the upper temperature limit of the experiments.

The bath gas densities (helium with up to 5% of radical precursors) of 3 × 10^{16} and 12 × 10^{16} molecules cm^{-3} were used in the room-temperature experiments and the density of 12 × 10^{16} molecules cm^{-3} was used at 400 and 520 K. Experimental parameters such as the photolyzing laser intensity and the concentrations of oxalyl chloride and cyclohexane were varied for individual experiments. For each temperature, the values of the $k_1[R]_0$ product obtained under different experimental conditions (including different bath gas densities) are shown on the same $k_1[R]_0$ versus $[R]_0$ plots in Figures 1 and 2. The rate constant of the cyclohexyl radical self-reaction does not demonstrate any dependence (within the experimental uncertainties) on the parameters varied; no pressure dependence of k_1 at room temperature can be observed within the experimental uncertainties. The conditions and the results of individual experiments are presented in Table 1. The values of k_1 determined from the slopes of the $k_1[R]_0$ versus $[R]_0$ dependences are also given in Table 1 for the three experimental temperatures.

The values of the rate constant obtained in the experiments are presented in Figure 3 as a function of temperature. A negative temperature dependence is observed, which can be represented with the following Arrhenius expression:

$$k_1 = 4.8 \times 10^{-12} \exp(+542\ \mathrm{K}/T)\ \mathrm{cm}^3\ \mathrm{molecule}^{-1}\mathrm{s}^{-1}\ (303-520\ \mathrm{K}) \quad \text{(II)}$$

Estimated uncertainty associated with this expression is 16% throughout the above temperature range.

Product Analysis. Formation of both $C_{12}H_{22}$ (m/z = 166) and C_6H_{10} (m/z = 82) was observed in real-time experiments, with the characteristic rise times matching those of the cyclohexyl decay due to reaction 1; these products were attributed to reaction channels 1a and 1b, respectively. An example of a C_6H_{10} growth profile and the corresponding C_6H_{11} decay is given in the Supporting Information. It was not possible to measure the ratio of these two products because of the difficulty in calibrating the sensitivity of the apparatus to $C_{12}H_{22}$ due to the very low vapor pressure of the latter. Instead, experiments to determine the ratio of the C_6H_{10} product concentration to the amount of HCl produced in reaction 3 were performed. These experiments were complicated by the fact that the intensity of the chlorine photoionizing lamp used to detect C_6H_{10} changed with time because of decreasing transparency of the CaF_2 windows during the experiment. To circumvent this problem, benzene was used as an internal standard. Measured low concentrations of benzene ((0.2−1.4) × 10^{13} molecules cm^{-3}, at least 18 times lower than the concentrations of cyclohexane to ensure that any potential contribution of the Cl + C_6H_6 reaction is negligible) were added to the reactive mixtures. The cyclohexene-to-benzene (with the chlorine lamp) and benzene-to-HCl (with the neon lamp) sensitivity ratios were determined experimentally using known concentrations of these species. Experiments were performed to verify that no photolysis of benzene occurs to any measurable extent. Recorded temporal profiles of the C_6H_{10} signal were fitted with a rising function obtained by numerical integration of the differential equation $d[C_6H_{10}]/dt = -k_{1b}[c\text{-}C_6H_{11}]^2$, where $[c\text{-}C_6H_{11}]$ is given by eq I, using the branching fraction of disproportionation $\gamma(1b) = k_{1b}/(k_{1a} + k_{1b})$ as the fitting parameter. The results are presented in Table 2. The quoted values of $[c\text{-}C_6H_{10}]_\infty$ given in the table are the infinite-time concentrations obtained by multiplying the initial radical concentration by the values of $\gamma(1b)$.

When branching fraction experiments were attempted at temperatures of 400 and 520 K, enhanced signals at m/z = 36 were observed when benzene was present in addition to hydrogen chloride, and a high-energy neon lamp with a collimated hole structure window was used. This effect was tentatively attributed to either production of HCl^+ or C_3^+ in ion−molecular reactions in the ion source or to C_3^+ fragment of $C_6H_6^+$. The latter could have appeared as a result of ionization of benzene with the higher-energy light from the neon lamp (unlike salt windows, the collimated hole structure does not block any low wavelength components) or from electron-impact ionization, with electrons generated by photoelectric effect due to light impacting the ion lenses. This m/z = 36 signal effectively prevented experiments on the branching fraction of channel 1b at temperatures above ambient. Thus, determination of the fraction of the reaction channel 1b was limited to room temperature. The results of these experiments are summarized in Table 2. The average value of the channel 1b branching fraction is 41 ± 7%, where the uncertainty includes 1σ random and systematic contributions. Attempts to determine the higher-temperature branching ratio of reaction 1 via final product analysis by gas chromatography were undertaken

Table 1. Conditions and Results of Experiments to Determine k_1

[M][a]	I[b]	[c-C_6H_{12}][c]	[$(CClO)_2$][c]	[c-C_6H_{11}]$_0$[d]	k_1[R]$_0$[e]	k_4[f]
Experiments at 303 ± 4 K. k_1(303 K) = (2.89 ± 0.43[g]) × 10^{-11} cm^3 molecule^{-1} s^{-1}						
12.0	8.9	2.62	0.65	1.86 ± 0.57	58.1 ± 3.6	10.7 ± 1.3
3.0	7.8	10.7	0.91	2.29 ± 0.31	74.3 ± 9.5	22.7 ± 3.3
12.0	9.0	2.62	1.15	3.33 ± 0.62	88.5 ± 5.4	12.7 ± 0.8
3.0	5.2	10.9	2.06	3.43 ± 0.63	91.6 ± 5.9	13.4 ± 0.9
12.0	14	2.67	0.87	3.99 ± 0.81	103 ± 7	9.7 ± 0.8
12.0	10	8.16	1.36	4.43 ± 0.76	132 ± 12	10.1 ± 1.2
12.0	11	2.62	1.36	4.60 ± 0.47	149 ± 15	10.7 ± 1.5
12.0	13	2.67	1.60	6.49 ± 1.07	179 ± 18	11.0 ± 0.8
3.0	5.0	10.9	4.17	6.76 ± 0.87	211 ± 28	13.1 ± 1.3
12.0	16	2.58	1.65	8.40 ± 1.39	237 ± 31	10.8 ± 0.8
3.0	13	2.04	2.45	9.89 ± 0.87	284 ± 52	23.8 ± 1.5
Experiments at 400 K. k_1(400 K) = (1.91 ± 0.28[g]) × 10^{-11} cm^3 molecule^{-1} s^{-1}						
12.0	3.1	2.94	2.19	2.15 ± 0.35	42.7 ± 2.7	9.9 ± 1.5
12.0	2.4	2.49	4.15	3.16 ± 0.32	65.0 ± 5.1	11.2 ± 1.8
12.0	2.3	5.81	6.36	4.66 ± 0.23	101 ± 8	10.0 ± 1.5
12.0	3.2	2.76	5.65	5.74 ± 0.26	95.1 ± 6.2	10.8 ± 0.9
12.0	3.2	2.97	8.36	8.71 ± 1.32	149 ± 17	9.9 ± 1.8
12.0	2.9	2.95	9.44	8.79 ± 0.56	186 ± 21	5.3 ± 1.1
Experiments at 520 K. k_1(520 K) = (1.34 ± 0.17[g]) × 10^{-11} cm^3 molecule^{-1} s^{-1}						
12.0	2.1	2.58	1.85	1.81 ± 0.50	19.1 ± 1.8	14.1 ± 2.0
12.0	2.6	2.75	2.52	2.15 ± 0.05	29.3 ± 1.7	13.3 ± 1.2
12.0	2.3	2.75	4.56	3.34 ± 0.06	38.5 ± 2.5	11.6 ± 1.5
12.0	2.7	2.85	6.92	6.06 ± 0.69	98.9 ± 6.9	11.0 ± 1.0
12.0	2.2	3.01	5.52	3.82 ± 0.19	53.8 ± 3.0	12.6 ± 1.1
12.0	3.3	3.09	8.24	8.67 ± 0.45	105.4 ± 9.8	15.6 ± 1.8

[a] Concentration of the bath gas (helium with up to 5% of radical precursors) in units of 10^{16} molecules cm^{-3}. [b] Estimated laser fluence in units of mJ pulse^{-1} cm^{-2}. [c] In units of 10^{14} molecules cm^{-3}. [d] Nascent concentration of cyclohexyl radicals in units of 10^{12} molecules cm^{-3} determined from production of HCl. [e] Obtained from the fits of the kinetics of the cyclohexyl decay with eq I. [f] Rate constant of the heterogeneous wall loss obtained from the fits of the kinetics of the c-C_6H_{11} decay with eq I. [g] Uncertainties are 1σ (statistical) + systematic.

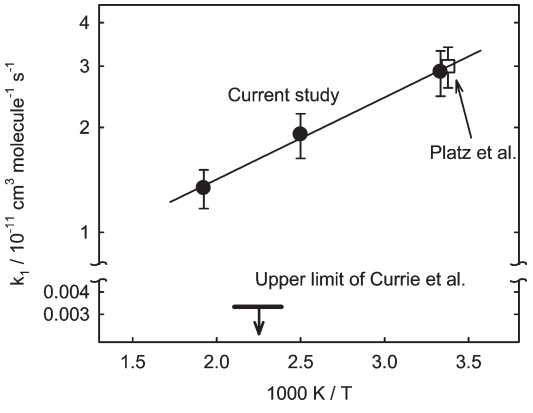

Figure 3. Temperature dependence of k_1. Filled circles: current study; open square: ref 6; wide horizontal line with a downward arrow: upper limit of ref 10.

but failed because of the reaction between the remaining oxalyl chloride and the gas chromatography column coating.

The sources of error in the measured experimental parameters such as temperature, pressure, flow rate, signal count, etc. were subdivided into statistical and systematic and propagated to the final values of the rate constants and branching ratios using different mathematical procedures for propagating systematic and statistical uncertainties.[24] The error limits of the values reported in this work represent a sum of 1σ statistical uncertainty and estimated systematic uncertainty, unless specified otherwise.

Table 2. Conditions and Results of Experiments to Determine the Branching Fraction of Disproportionation in Reaction 1[a]

T/K	[c-C_6H_{12}][b]	[$(CClO)_2$][b]	[c-C_6H_{11}]$_0$[c]	[c-C_6H_{10}]$_\infty$[d]	γ(1b)[e]
305	2.54	1.56	2.08 ± 0.16	0.84 ± 0.07	40.4 ± 6.0%
305	2.54	2.50	3.20 ± 0.34	1.19 ± 0.11	37.2 ± 6.7%
306	2.51	5.32	5.76 ± 0.41	2.59 ± 0.20	45.0 ± 4.2%

[a] All quoted uncertainties are 1σ (statistical) + systematic. [b] In units of 10^{14} molecules cm^{-3}. [c] Nascent concentration of cyclohexyl radicals in units of 10^{12} molecules cm^{-3} determined from production of HCl. [d] Concentration of cyclohexene extrapolated to infinite time (see text), in units of 10^{12} molecules cm^{-3}. [e] Branching fraction of channel 1b.

III. DISCUSSION

This work presents the first direct real-time experimental determination of the rate constant of the c-C_6H_{11} + c-C_6H_{11}

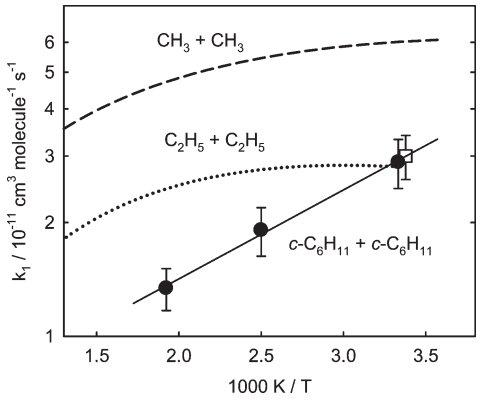

Figure 4. Temperature dependence of k_1 (symbols and solid line, as in Figure 3) compared with the temperature dependences of the rate constants of the self-reactions of CH_3 (dashed line, theory-based parametrization of ref 4) and C_2H_5 (dotted line, ref 5).

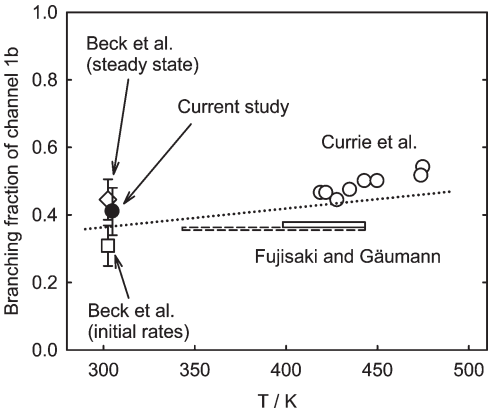

Figure 5. Values of the branching fraction of the disproportionation channel (1b) obtained at different temperatures. Filled solid circle: current study; open square and open diamond: ref 9, values derived from the initial product formation rates and from the steady-state cyclohexene formation rate, respectively; open circles: ref 10; narrow long rectangles with dashed and solid line borders: refs 11 and 12, respectively. Straight dotted line: a least-squares linear fit to the temperature dependence (see text).

reaction (k_1) as a function of temperature (303−520 K). The overall rate constant values obtained in the current study are in agreement with the earlier room-temperature value of k_1 reported by Platz et al.[6] (Figure 3). The 1.7×10^{-14} cm^3 molecule^{-1} s^{-1} upper limit given by Currie et al.[10] for the rate constant of the recombination channel 1a and corresponding to the upper limit of $\sim 3 \times 10^{-14}$ cm^3 molecule^{-1} s^{-1} for the overall reaction is more than 2 orders of magnitude lower than the results of the current study. This upper limit was obtained by the authors of ref 10 in their analysis of the final products of a system of reactions occurring during 360-nm photolysis of azocyclohexane in the presence of carbon tetrachloride and cyclohexane. The main focus of that study was the kinetics of the reactions of cyclohexyl radicals with CCl_4 and that of the CCl_3 radicals with cyclohexane. Rates of some of the reactions playing important roles in the experimental system were unknown and had to be estimated by the authors. The uncertainties of these estimates have likely affected the resulting evaluation of k_{1b}. In particular, a rather low upper limit of 6.6×10^{-13} cm^3 molecule^{-1} s^{-1} to the preexponential factor of the abstraction reaction of the cyclohexyl radicals with CCl_4 was assumed, which, combined with experimentally determined product ratios, translated into a low value of 5×10^{-13} cm^3 molecule^{-1} s^{-1} for the upper-limit rate constant of the c-C_6H_{11} + CCl_3 cross-combination reaction. The latter value was converted into the $k_{1a} \leq 1.7 \times 10^{-14}$ cm^3 molecule^{-1} s^{-1} upper limit by using an experimentally determined cross-combination-to-recombination products ratio of c-C_6H_{11} and CCl_3 and a literature value for the rate constant of CCl_3 recombination.

It is interesting to note that the rate of reaction 1 demonstrates rather strong negative temperature dependence (Figures 3 and 4). Figure 4 compares the temperature dependence of k_1 with those of the self-reactions of methyl and ethyl radicals, the only two alkyl radical self-reactions for which directly determined temperature-dependent rate constants are available in the literature. As can be seen from the plot, within the 303−520 K temperature range, the rate constant of reaction 1 decreases with temperature much faster than the rates of self-reactions of the other two smaller radicals. In that respect, reaction 1, with a negative activation energy of −4.51 kJ mol^{-1} (E/R = −542 K, eq II), behaves in a manner similar to that of the reactions of small alkyl radicals (C_2H_5, n-C_3H_7, and n-C_4H_9) with CH_3, which have reported negative activation energies in the −3.93 to −1.62 kJ mol^{-1} range (E/R between −473 K and −387).[25] The difference between the temperature dependence of reaction 1 and those of methyl and ethyl radical self-reactions is in general agreement with the observation by Klippenstein et al.[4] that additional substituents at the radical center and increasing steric bulk of radicals result in stronger negative temperature dependences of their theoretically calculated recombination rate constants.

Figure 5 presents the branching fraction of the disproportionation channel (1b) obtained in the current study in comparison with the values reported in or derived from the results of earlier relative-rates studies, as explained below. The branching fraction values are shown as a function of temperature.

In 1954, Beck et al.[9] used mercury-photosensitized decomposition of cyclohexane at 302 K to produce cyclohexyl radicals and H atoms under static reactor conditions and gas chromatography/mass spectrometry to identify and quantify the products of the subsequent reactions. The initial rates of product formation and those obtained under steady-state conditions were determined; the authors reported a value of 2.2 for the recombination-to-disproportionation branching fraction obtained from the initial rates. Using this value and the uncertainties given for the rates of product formation in ref 9, one can obtain a value of 31 ± 6% for the fraction of channel 1b (open square in Figure 5). The authors comment that product formation rates of cyclohexene and hydrogen obtained experimentally under steady-state conditions are somewhat lower than expected from the analysis of the initial rates. Using the steady-state rate of cyclohexene formation within the framework of the mechanism of ref 9 yields a higher value of the disproportionation branching fraction, 45 ± 6% (calculated in the current study), which is shown in Figure 5 with an open diamond.

In 1974, Currie et al.[10] used 360 nm photolysis of mixtures of azocyclohexane, carbon tetrachloride, and cyclohexane to produce c-C_6H_{11} and gas chromatography and mass spectrometry to analyze final products. Formation of both bicyclohexane and cyclohexene, attributed to reactions 1a and 1b, was observed and quantified. The authors did not use these results to evaluate the branching ratio of reaction 1; instead, they referred in the article to their earlier (apparently, unpublished) study in which the disproportionation to combination ratio of 0.99 was obtained, with no error limits given. Using the reported[10] yields of $C_{12}H_{22}$

and c-C_6H_{10}, one can obtain similar values (averaging to 0.94 at T = 419−475 K), although with a positive temperature dependence. Open circles in Figure 5 show the corresponding values of the fraction of the disproportionation channel.

In 1979, Fujisaki and Gäumann[11] used radiolysis of water vapor in the presence of cyclohexane and final analysis of products by gas chromatography to determine the disproportionation-to-combination ratio of reaction 1. The value of 0.56 ± 0.01 was reported for the 343−443 K experimental range of temperatures. In 1982, the same authors repeated their experiments using somewhat different experimental conditions, as a part of their study of self-reactions and cross-radical reactions involving cyclohexyl and cyclopentyl radicals, as well as their deuterated analogues.[12] The temperature range of the second study was more narrow (398−443 K), and the reported disproportionation-to-combination ratio value was 0.59 ± 0.02. The corresponding values of the disproportionation branching fraction are 35.9 ± 0.4% and 37.1 ± 0.8% for the 1979 and the 1982 studies, respectively. These envelopes of uncertainties are shown in Figure 5 with thin long rectangles covering the associated temperature ranges and framed with dashed and solid lines.

The values of the channel 1b branching fraction shown in Figure 5 are in general agreement with each other, covering the range of roughly 30−50%. The general trend, together with the results of Currie et al. seems to suggest a weak positive temperature dependence. Drawing a least-squares linear fit through the data results in the following equation for the disproportionation branching fraction: $\gamma(1b) = 20 + 0.056 \times T$ %, shown in Figure 1 with a dotted line. However, the scatter of the data exceeds variation in $\gamma(1b)$ within the temperature range covered by experiments due to this hypothetical trend, and thus it may be preferable to use the room-temperature value of the current study, 41 ± 7%, for all temperatures instead. The corresponding temperature dependences of the recombination and the disproportionation channels are

$$k(1a) = 2.8 \times 10^{-12} \exp(+542\ \mathrm{K}/T)\ \mathrm{cm^3\ molecule^{-1}\ s^{-1}}\ (303-520\ \mathrm{K}) \quad \text{(III)}$$

$$k(1b) = 2.0 \times 10^{-12} \exp(+542\ \mathrm{K}/T)\ \mathrm{cm^3\ molecule^{-1}\ s^{-1}}\ (303-520\ \mathrm{K}) \quad \text{(IV)}$$

with estimated uncertainties of 20% and 29%, respectively.

■ ASSOCIATED CONTENT

Supporting Information. A supplement, including a full-sized plot of the dependence given in the lower right inset of Figure 1 (Figure 1S) and an example of a C_6H_{10} growth profile and the corresponding C_6H_{11} decay (Figure 2S). This material is available free of charge via the Internet at http://pubs.acs.org.

■ AUTHOR INFORMATION

Corresponding Author
*E-mail: knyazev@cua.edu.

■ ACKNOWLEDGMENT

This research was supported by the U.S. National Science Foundation's Combustion, Fire, and Plasma Systems Program under Grant No CBET-0853706.

■ REFERENCES

(1) Tsang, W.; Hampson, R. F. *J. Phys. Chem. Ref. Data* **1986**, *15*, 1087.
(2) Warnatz, J.; Mass, U.; Dibble, R. W. *Combustion: Physical and Chemical Fundamentals, Modeling and Simulation, Experiments, Pollutant Formation*; Springer: Berlin/Heidelberg/New York, 1996.
(3) Georgievskii, Y.; Miller, J. A.; Klippenstein, S. J. *Phys. Chem. Chem. Phys.* **2007**, *9*, 4259.
(4) Klippenstein, S. J.; Georgievskii, Y.; Harding, L. B. *Phys. Chem. Chem. Phys.* **2006**, *8*, 1133.
(5) Shafir, E. V.; Slagle, I. R.; Knyazev, V. D. *J. Phys. Chem. A* **2003**, *107*, 871.
(6) Platz, J.; Sehested, J.; Nielsen, O. J.; Wallington, T. J. *J. Phys. Chem. A* **1999**, *103*, 2688.
(7) Baklanov, A. V.; Krasnoperov, L. N. *J. Phys. Chem. A* **2001**, *105*, 97.
(8) Shafir, E. V.; Slagle, I. R.; Knyazev, V. D. *J. Phys. Chem. A* **2003**, *107*, 8893.
(9) Beck, P. W.; Kniebes, D. V.; Gunning, H. E. *J. Chem. Phys.* **1954**, *22*, 672.
(10) Currie, J.; Sidebottom, H.; Tedder, J. *Int. J. Chem. Kinet.* **1974**, *6*, 481.
(11) Fujisaki, N.; Gäumann, T. *Int. J. Chem. Kinet.* **1979**, *11*, 345.
(12) Fujisaki, N.; Gäumann, T. *Int. J. Chem. Kinet.* **1982**, *14*, 1059.
(13) Slagle, I. R.; Gutman, D. *J. Am. Chem. Soc.* **1985**, *107*, 5342.
(14) Niiranen, J. T.; Gutman, D.; Krasnoperov, L. N. *J. Phys. Chem.* **1992**, *96*, 5881.
(15) Baklanov, A. V.; Krasnoperov, L. N. *J. Phys. Chem. A* **2001**, *105*, 4917.
(16) Hooshiyar, P. A.; Niki, H. *Int. J. Chem. Kinet.* **1995**, *27*, 1197.
(17) Russell, J. J.; Seetula, J. A.; Senkan, S. M.; Gutman, D. *Int. J. Chem. Kinet.* **1988**, *20*, 759.
(18) Slagle, I. R.; Gutman, D.; Davies, J. W.; Pilling, M. J. *J. Phys. Chem.* **1988**, *92*, 2455.
(19) Sirjean, B.; Glaude, P. A.; Ruiz-Lopez, M. F.; Fournet, R. *J. Phys. Chem. A* **2008**, *112*, 11598.
(20) Knepp, A. M.; Meloni, G.; Jusinski, L. E.; Taatjes, C. A.; Cavallotti, C.; Klippenstein, S. J. *Phys. Chem. Chem. Phys.* **2007**, *9*, 4315.
(21) Gilbert, R. G.; Smith, S. C. *Theory of Unimolecular and Recombination Reactions*; Blackwell: Oxford, 1990.
(22) Holbrook, K. A.; Pilling, M. J.; Robertson, S. H. *Unimolecular Reactions*, 2nd ed.; Wiley: New York, 1996.
(23) Mokrushin, V.; Bedanov, V.; Tsang, W.; Zachariah, M. R.; Knyazev, V. D.; McGivern, W. S. *ChemRate*, version 1.5.8; National Institute of Standards and Technology: Gaithersburg, MD, 2011 (http://kinetics.nist.gov/chemrate/).
(24) Colclough, A. R. *J. Res. Natl. Bur. Stand.* **1987**, *92*, 167.
(25) Knyazev, V. D.; Slagle, I. R. *J. Phys. Chem. A* **2001**, *105*, 6490.